24 GHz Indoor MIMO Channel Measurements

Rashid Mehmood, Jon W. Wallace, and Michael A. Jensen
Electrical and Computer Engineering, Brigham Young University, USA
E-mail: {r.mehmood,wall}@ieee.org, jensen@byu.edu

***Abstract*—The demand for increased bandwidth to support modern mobile wireless services has pushed the community to explore higher carrier frequencies where spectrum is more readily available. However, relatively few studies have focused attention on bands such as 24 GHz that may support non-line-of-sight communication. This paper provides experimental measurements of multi-antenna, wideband propagation channels at 24 GHz, with emphasis on observed delay spreads, pathloss, and achieved capacity for different channel conditions.**

I. INTRODUCTION

Because of the widespread use of frequencies between 400 MHz and 6 GHz for mobile wireless communications, a huge volume of work has appeared characterizing the electromagnetic propagation at these frequencies in a wide variety of different settings [1, 2]. However, with interest in having access to larger frequency bandwidths to satisfy increased demand for data-intensive applications, significant focus has turned to understanding millimeter-wave bands, with particular emphasis on communication around 60 GHz [3]. While such frequencies are suitable for line-of-sight (LOS) communication, many applications require high-bandwidth capabilities for non-line-of-sight (NLOS) scenarios, motivating exploration of frequencies near 24 GHz where large bandwidths are available but NLOS communication may still be possible. To date, however, only limited studies of the propagation in such bands have appeared [4, 5], particularly for multiple-input multiple-output (MIMO) communication. This paper reports on an experimental MIMO channel sounding platform offering 500 MHz of bandwidth at 24 GHz. Representative measurement results in an indoor environment show power delay profiles (PDP), delay spread, pathloss and channel capacity.

II. MEASUREMENT SETUP

Figure 1 shows the system-level block diagram of the custom MIMO channel sounder used in this work. The receive (Rx) node generates a frequency-modulated continuous-wave (FMCW) signal (chirp) with a 250 MHz bandwidth centered at 12 GHz and a 1 ms sweep time. This signal is routed through a frequency doubler to achieve a signal with a 500 MHz bandwidth at a center frequency of 24 GHz that modulates an optical carrier by means of an optical transmitter (OT). The optical signal is sent over a 35 m length of optical fiber (OF) to an optical receiver (OR) that recovers the original 24 GHz signal at the transmit (Tx) node. This signal, whose power is approximately -8 dBm, is amplified and fed to a signal-pole four-throw (SP4T) switch that routes the signal to one of the N_{T} power amplifier/transmit antenna combinations. Variable attenuation is placed in the transmit amplifier path to allow transmit powers at the antenna terminals between -25 dBm and $+25$ dBm.

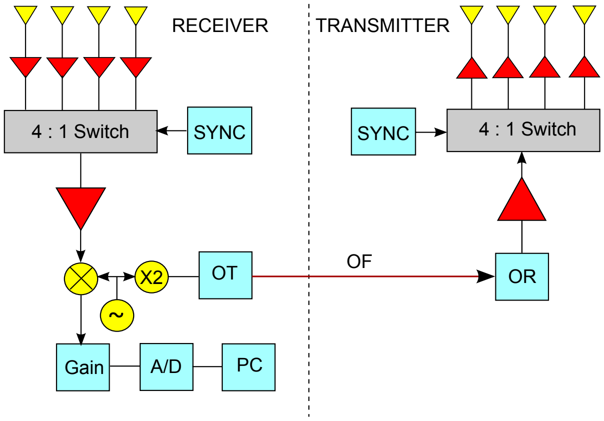

Fig. 1. System level diagram of MIMO channel sounder

The signal received from each of the N_{R} Rx antennas passes through a low-noise amplifier (LNA) to a SP4T switch. Following a second LNA stage, for a total Rx RF gain of 34 dB (includes circuit losses), a subharmonic mixer multiplies the 24 GHz received signal with the 12 GHz chirp. The resulting baseband signal is amplified (40 dB) and sampled at 1 Msample/s using a 16-bit A/D converter. The sampled data is processed on a personal computer (PC).

Each SYNC unit shown in Fig. 1 consists of an FPGA clocked by a disciplined rubidium reference [6]. The control logic sequentially connects the signal to each of the N_{T} Tx antennas for the 1 ms chirp duration as well as inserts a 1 ms *blank* (no transmit signal) to allow for synchronization of the Tx and Rx SYNC units. Upon completion of this cycle of $N_{\mathrm{T}}+1$ transmit periods, the Rx SYNC unit switches another of the N_{R} Rx antennas to the Rx chain, and the transmitter repeats its cycle. This allows measurement of the channel for all Tx/Rx antenna pairs over a duration of $(N_{\mathrm{T}}+1)N_{\mathrm{R}}$ ms. The measurements reported here use vertically-polarized slot antennas that have a reflection coefficient of less than -10 dB over the frequency range of 23-25 GHz.

III. MEASURED RESULTS

Measurements with the system were performed using $N_{\mathrm{T}} = 3$ Tx and $N_{\mathrm{R}} = 4$ Rx antennas on the 5th floor of the Clyde Engineering Building on the Brigham Young University campus. Figure 2 shows the map of the environment along with the fixed Rx location and the route followed by the Tx node. The rooms have cinderblock walls and contain lab benches outfitted with metal shelving that rises to a height of approximately 2.5 m. The Tx route from locations 1 to 2 is along a corridor between these benches, and as the Rx

978-1-4799-7815-1/15/$31.00 ©2015 IEEE

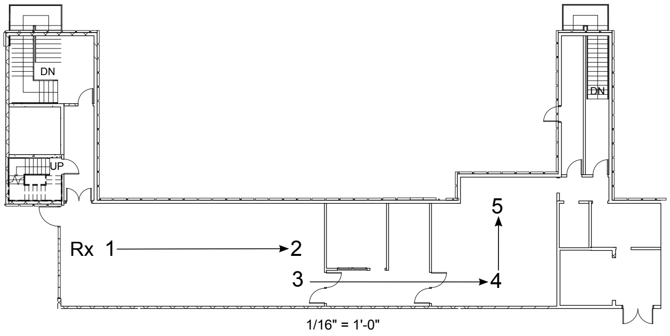

Fig. 2. Position of the Rx node and route followed by the Tx node, where arrows correspond to the direction of movement.

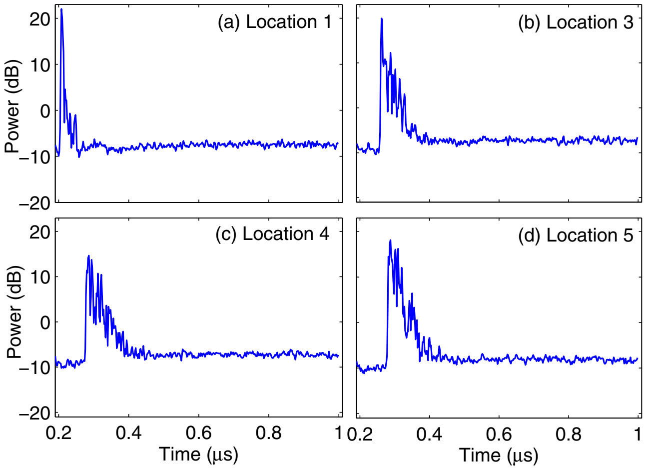

Fig. 3. Received power versus delay at four different transmit locations: (a) Location 1 (1.2 m); (b) Location 3 (11.2 m); (c) Location 4 (20.5 m); (d) Location 5 (26.5 m).

moves through the first doorway from location 3, the channel transitions from LOS to NLOS. A channel measurement is captured every time the Tx moves 0.3 m.

Figure 3 plots the PDP, which is the received power as a function of delay, at four of the Tx locations. A Hamming window is applied to the frequency domain data before it is processed via a fast Fourier transform to the delay domain. The peak signal-to-noise ratio (SNR) in these plots is around 35 dB, although it varies somewhat over the measurement range due to the adaptive transmit signal amplification. Figure 4(a) plots the root mean square delay spread τ averaged over all Tx/Rx antenna combinations as a function of Tx position along the route, where the computation ignores values below the noise floor and lines designate numbered Tx locations. As expected, τ increases with an increase in separation between the Tx and Rx nodes, consistent with the transition from LOS to NLOS propagation. Figure 4(b) plots the relative received power (inverse of pathloss), with the results demonstrating dramatic increases in the pathloss as the Tx moves through doorways. Despite this, however, the propagation at this frequency can offer reasonable NLOS received signal strengths. Finally, Table I shows the uninformed transmitter capacity for the 4×3 MIMO system assuming an SNR of 10 dB at four different Tx locations, where the increased multipath richness created by increased Tx-Rx separation creates an increase in the capacity (note that SNR decreases are ignored due to the channel normalization).

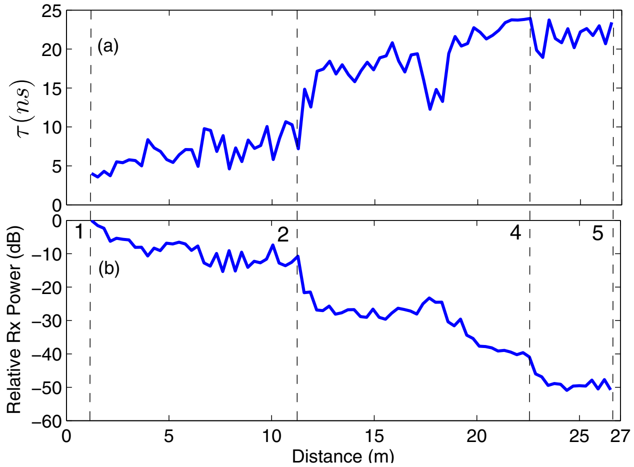

Fig. 4. (a) Delay spread as a function of distance between Tx and Rx nodes. (b) Relative received power as a function of distance between the Tx and Rx nodes, where dashed lines mark various transmit locations.

TABLE I
MIMO CAPACITY AT DIFFERENT TX LOCATIONS

Tx Location	Capacity (bits/s/Hz)
1	6.171
2	7.519
4	7.915
5	7.686

IV. CONCLUSIONS

This paper reports on an experimental MIMO channel sounder that can measure up to 500 MHz of bandwidth at a center frequency of 24 GHz. Measurements of a 4×3 MIMO channel in an indoor environment reveal the PDP and resulting delay spread, pathloss, and MIMO capacity for the environment. The results demonstrate that such a frequency can support NLOS communication.

REFERENCES

[1] M. A. Jensen and J. W. Wallace, "A review of antennas and propagation for MIMO wireless communications," *IEEE Trans. Antennas Propag.*, vol. 52, pp. 2810–2824, Nov. 2004.

[2] R. Vaughan and J. B. Andersen, *Channels, Propagation, and Antennas for Mobile Communications*, The Institution of Electrical Engineers, London, 2003.

[3] P. Smulders, "Exploiting the 60 GHz band for local wireless multimedia access: prospects and future directions," *IEEE Communications Mag.*, vol. 40, pp. 140–147, Jan. 2002.

[4] D. Lu and D. Rutledge, "Investigation of indoor radio channels from 2.4 GHz to 24 GHz," in *IEEE Antennas and Propag. Soc. Intl. Symp.*, Columbus, OH, 22-27 Jun. 2003, vol. 2, pp. 134–137.

[5] O. J. Femi-Jemilohun, T. Quinlan, S. Barc, and S. D. Walker, "An experimental investigation into GbE wireless data communication at 24 GHz in non-line-of-sight and multipath rich environments," *IEEE Antennas Wireless Propag. Lett.*, vol. 13, pp. 1219–1222, 2014.

[6] B. T. Maharaj, J. W. Wallace, M. A. Jensen, and L. P. Linde, "A low-cost open-hardware wideband multiple-input–multiple-output (MIMO) wireless channel sounder," *IEEE Transactions on Instrumentation and Measurement*, vol. 57, no. 10, pp. 2283–2289, 2008.